NDE X-RAY IMAGE ANALYSIS USING MATHEMATICAL MORPHOLOGY

Mathew S. Chackalackal and John P. Basart

Department of Electrical and Computer Engineering
Center for Nondestructive Evaluation
Iowa State University
Ames, IA 50011

INTRODUCTION

Morphology is the study of form and structure. In image processing, morphology refers to the analysis of structure or texture within an image. The basic principle in mathematical morphology is to probe the microstructure of the image with various geometric structures to extract features of interest from the image. These geometric structures are known as structuring elements.

Morphological techniques are used in a variety of areas, including medical imaging and cellular biology. However, in the area of nondestructive evaluation, the application of morphological image processing is in its infancy. In our research program, we have developed various morphological routines and applied them to low contrast x-ray images. These applications include estimating and reducing the background in images, reducing random noise, enhancing images, eliminating artifacts, and detecting cracks and boundaries.

The principles of mathematical morphology are based on set theory and Minkowski algebra. In this paper we describe very briefly the principles of mathematical morphology and then discuss its applications in analysis of x-ray images. Further information can be found in Dougherty and Giardina [1], and in Serra [2].

In the following material we briefly state the definitions of the basic morphological operations. A and B in Euclidean space represent the image and the structuring element, respectively.

BINARY MORPHOLOGY

Translation: For an element x of Euclidean space, the translation of A by x [1] is defined by

$$A + x = \{a + x: a \in A\} \qquad (1)$$

where "+" denotes vector addition and A is a set of points. A translated by x is denoted by $(A)_x$.

Review of Progress in Quantitative Nondestructive Evaluation, Vol. 9
Edited by D.O. Thompson and D.E. Chimenti
Plenum Press, New York, 1990

Dilation: The dilation of A by B is given by [2]

$$A \oplus B = \{c \mid c = a + b \text{ for some } a \in A \text{ and } b \in B\} \text{ or } \bigcup_{b \in B} (A)_b \quad (2)$$

where " " denotes dilation. Dilation is a growing operation. The growth of A depends on the size and shape of B.

Erosion: The erosion of A by B is given by

$$A \ominus B = \{c \mid c + b \in A \text{ for every } b \in B\} \text{ or } \bigcap_{b \in B} (A)_b \quad (3)$$

where " " denotes erosion. Erosion is a shrinking operation.

GRAY SCALE MORPHOLOGY

It is possible to perform erosion and dilation on gray scale images [1,2,3,4,5]. The structuring elements used in this case are three dimensional structures such as hemispheres, cones, cylinders, etc. [5]. The third dimension is the image intensity.

Dilation: The function defining the surface of the image C, obtained by dilating A by B is given by [1,3]

$$c(x,y) = \max_{i,j}\{a(x - i, y - j) + b(i,j)\} \quad (4)$$

where c(x,y) is the gray scale intensity of the dilated image at (x,y) and i x j is the size of B.

Erosion: The function defining the surface of the image C, obtained by dilating A by B is given by [3]

$$c(x,y) = \min_{i,j}\{a(x - i, y - j) - b(i,j)\} \quad (5)$$

where c(x,y) is the gray scale intensity of the dilated image at (x,y) and i x j is the size of B.

MORPHOLOGICAL FILTERS

The lack of duality between erosion and dilation is exploited by the two morphological filtering operations, opening and closing.

Opening: Opening of A by B is defined by [4,5]

$$O(A,B) = ((A \ominus B) \oplus B) \quad (6)$$

Eroding A by B removes all of the bright regions in A that are smaller than the structuring element (B). The bright regions in A that are bigger than B shrink in size. Now, dilating the eroded image by B expands all those shrunk regions back to normal size. But, all those regions that were removed by erosion can not be restored. Thus, opening is a nonlinear filtering operation that removes bright features smaller than the structuring element from the image. Fig. 1 illustrates opening. All images displayed in this paper were digitized to 256 gray-scale levels. The picture on the left is the digitized x-ray radiograph of a composite material (contributed by Westinghouse). The picture on the right is the original opened by a 9 x 9 hemisphere, where 9 x 9 is the size of the mask used. The equation for the hemisphere is given by

$$z^2 = 12^2 - (12m/4)^2 - (12n/4)^2 \tag{7}$$

where z is the intensity at any point (m,n) in the hemisphere and 12 is the height of the hemisphere. In the above expression, m and n are local pixel coordinates whose origin is at the center of the 9 x 9 mask. The algorithm to generate the mask is given in Chackalackal and Basart [5].

Fig. 1(b) retains most of the image, save for the flaws. The size of the structuring element is critical. By using a sufficiently large enough structuring element, it is possible to pull out the entire flaw information. To be on the safe side a structuring element, which is about 5 pixels bigger than the largest flaw should be used.

Closing: Closing of A by B is defined by

$$C(A,B) = ((A \oplus B) \ominus B) \tag{8}$$

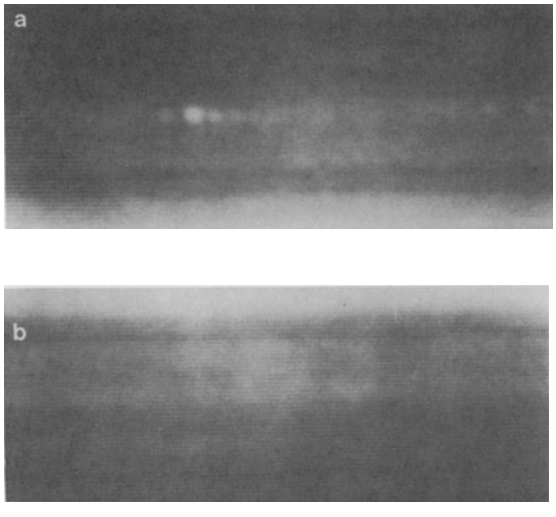

Fig. 1. (a) Original image. (b) Opened image.

Dilating A by B removes all of the dark regions in A that are smaller than the structuring element. The dark regions in A that are bigger than B shrink in size. Eroding the dilated image by B, expands all those shrunk regions back to normal size. All those regions removed by dilation can not be restored. Thus, closing is a nonlinear filtering operation that removes dark features smaller than the structuring element from the image.

Hybrid filtering: A combination of opening and closing can be used to reduce random noise from noisy images [1]. Noise may appear as black and white dots on the image. Closing and then opening by a small structuring element removes most of the noise-like features from the image. Fig. 2(a) shows the intensity versus position through a slice of an x-ray image. Fig. 2(b) shows a similar slice after hybrid filtering the image.

In Fig. 2(a), the dip in the slice representing the flaw is corrupted by noise. In Fig. 2(b), the dip representing the flaw stands out.

Hybrid filtering does a similar, but different, job than frequency domain filtering. For the original image in Fig. 2, low pass filtering would have given similar results. The fact that one can choose the size of the structuring element makes it possible to remove noise-like regions larger than 3 x 3 pixels that low-pass filtering may fail to remove completely.

ESTIMATION AND REDUCTION OF BACKGROUND

The most important application of morphological filters, opening and closing, to the field of NDE is in the estimation of backgrounds [5,6]. A background is defined to be the regions in an image that are not significant to the analyst. So, from the NDE point of view, the entire image excluding the flaws is the background. When flaws in an image are brighter than the background, then

$$\text{Background estimate (bkgr)} = A(\text{open})B \tag{9}$$

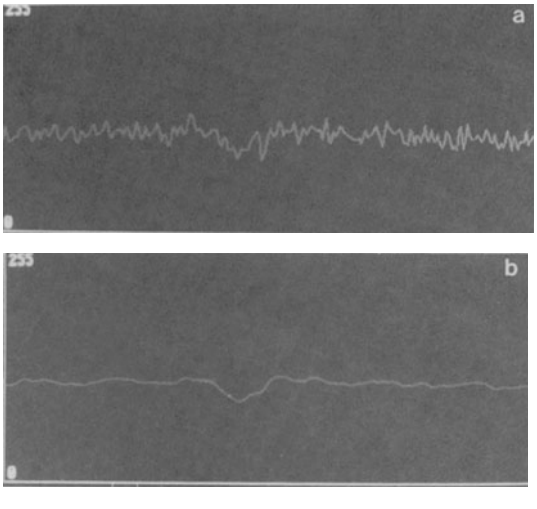

Fig. 2 (a) Slice through original image. (b) Slice through hybrid filtered image.

where B is a cylindrical structuring element [5] bigger than the size of the largest flaw in the image. Subtracting the background estimate from the original image can reduce the background considerably. The image shown in Fig. 1(b) is an estimate of the background of the image in Fig. 1(a). Subtracting Fig. 1(b) from Fig. 1(a) gives an image with a reduced background (Fig. 3).

In the background reduced image, the size of the flaws are approximately the same as in the original. The intensity has been multiplied by a factor of eight. The original image used in Fig. 3 has background trends, is not very noisy, and is ideal for background reduction. If the image happened to be noisy, the background-reduced image would have contained the noise too. Most of the noise can be removed by opening with a small structuring element and using the filtered image as the starting image. If the flaws are very small, then the structuring element would not be able to differentiate between noise and flaws. But once the noise and the flaws have been extracted, it may possible to remove the noise by thresholding.

When the flaws are darker than the image, then

$$\text{Background estimate} = A(\text{close})B \tag{10}$$

where B is bigger than the size of the largest flaw. Morphological filters can also be used for image enhancement [5]. For example, once the background is reduced, the flaws can be superimposed on a white background. Fig. 4(a) is the digitized x-ray image of a control valve, containing a flaw hidden in the transition region. Fig. 4(b) is the enhanced image obtained by closing the original with a 25 x 25 cylinder, reducing the background, and then superimposing it on a white background.

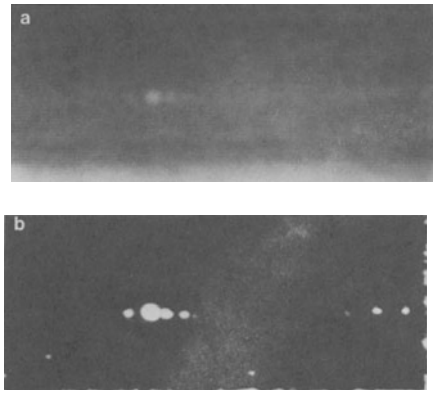

Fig. 3 (a) Original image. (b) Background reduced image.

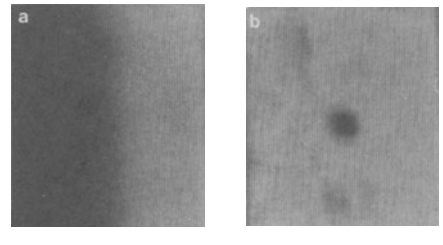

Fig. 4 (a) Original image. (b) Enhanced image.

Fig. 4 is an illustration of morphological filtering and image enhancement. Many of the image enhancement routines like histogram equalization and contrast stretching will not detect the flaw hidden in the transition region. Fig. 4 illustrates the power of morphology to extract faint flaws. This technique is very effective when the images are not very noisy, in which case it might pull out some noise too.

BOUNDARY DETECTION

The gradient can be defined [7] in terms of morphological operators as

$$\text{Gradient} = [A \oplus B] - [A \ominus B] \tag{11}$$

where A is the image and B is a 3 x 3 cylinder. The principle is pictorially represented in Fig. 5.

As can be seen from Fig. 5, the boundary is two pixels thick and might appear out of focus. A sharper boundary can be obtained by defining the gradient to be

$$\text{Gradient} = [A \oplus B] - A \tag{12}$$

An example of this operation is shown in Fig. 6. Fig. 6(a) is the digitized radiograph of a honeycomb structure (courtesy of Joe Gray). Fig. 6(b) is the boundary detected image.

In Fig. 6, the objective was to detect the signature of crushed core, which appears as a halo around the hexagonal structure of the honeycomb. In Fig. 6(b), the signature of the crushed core appears as lines parallel but very close to the hexagonal edges.

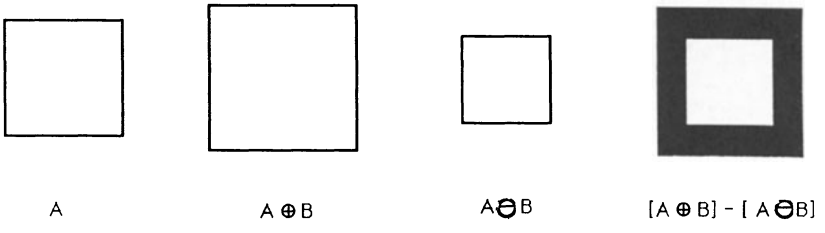

Fig. 5. Pictorial representation of gradient operation.

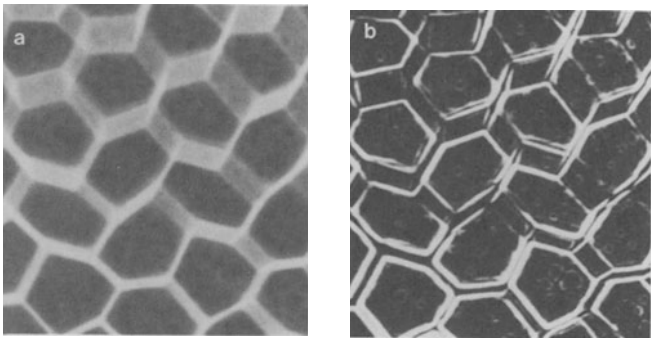

Fig. 6 (a) Original image. (b) Result of edge detection.

Boundary detection is a powerful tool for NDE applications. The Laplacian operator might give comparable results, but if the image happens to be noisy the Laplacian would amplify noise more than the morphological edge detector. The morphological edge detector detects very faint edges like those corresponding to crushed core in Fig. 6.

ELIMINATION OF ARTIFACTS

Many radiographs have artifacts that are often misleading or distort valuable information. When these artifacts are in the form of lines, opening or closing by planes can eliminate them. The horizontal and vertical structuring elements, denoted by H and V, respectively, are shown in Fig. 7. The length of the structuring element should be less than the length of the artifact.

Elimination of horizontal artifact = A(open or close)H (13)

Elimination of vertical artifact = A(open or close)V (14)

Fig. 8 shows an x-ray radiograph of a composite material (contributed by Westinghouse) with artifacts and the result of artifact elimination.

The two bright horizontal streaks in Fig. 8(a) are artifacts. The artifacts have been totally removed from the image. this can be largely attributed to the fact that the artifacts were perfectly horizontal. The image was opened by a plane of length 15 pixels to eliminate the artifacts. Eliminating the artifacts make the image a lot easier to work with. Diagonal structuring elements could be used for removing diagonal artifacts.

$$H = \underbrace{[\,1\ 1\ -\ -\ -\ 1\ 1\,]}_{a}{}_{1 \times 15} \qquad V = \underbrace{\begin{bmatrix} 1 \\ 1 \\ - \\ - \\ - \\ 1 \\ 1 \end{bmatrix}}_{b}{}_{15 \times 1}$$

Fig.7 (a) H. (b) V.

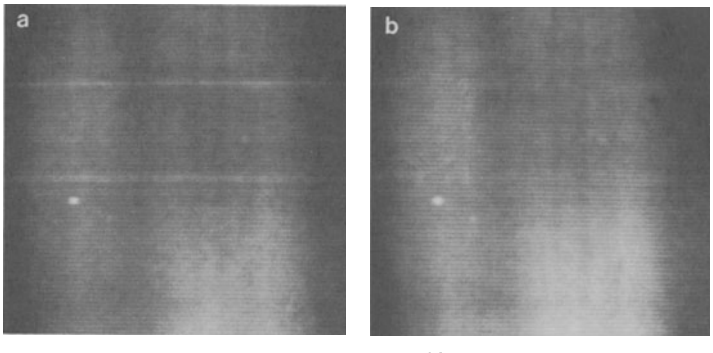

Fig. 8(a) Original Image. (b) Artifact Eliminated image.

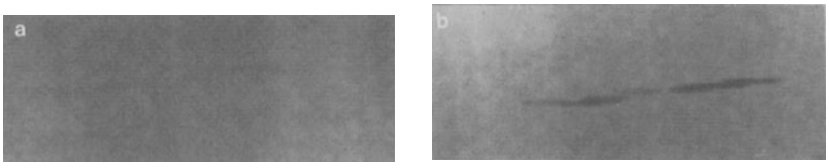

Fig. 9 (a) Original image. (b) Result of crack detection.

DETECTION OF CRACKS

The principle of elimination of artifacts can be extended to the detection of cracks. Closing the image with vertical or horizontal planes gives the background estimate. Reducing the background leaves the cracks behind. Fig. 9 gives the digitized x-ray radiograph of a pipe (contributed by Westinghouse) and the result of crack detection.

Fig. 9(a) has a faint horizontal flaw. The flaw is pulled out by closing with a plane of length 17 pixels and is then superimposed on the original image. The detected flaw is composed of linear segments. This technique is useful for flaw detection, but not for flaw characterization. This technique is very effective in pulling out faint crack like flaws. It could pull out a lot of noise if the image is very noisy.

CONCLUSION

The results discussed in this paper illustrate that morphological techniques can be used effectively to analyze X-ray NDE images. These techniques can also be applied to ultrasonic and eddy current images. The principle of reduction of background takes us a step closer in detecting flaws in complex images. It might be possible to estimate backgrounds using other techniques, but very few existing techniques are as simple and reliable as morphological filtering. Morphological edge detectors when compared to gradient edge detectors are less sensitive to noise and are comparable in speed with them. Morphological techniques are very reliable and invariably gives good results.

ACKNOWLEDGEMENT

This work was supported by the Center for NDE at Iowa State University and was performed at the Ames Laboratory. Ames Laboratory is operated for the U.S.Department of Energy by Iowa State University under Contract No.W-7405-ENG-82.

REFERENCES

1. Dougherty, E. R., Giardina, C. R., Morphological Methods in Image and Signal Processing, (Prentice Hall, New Jersey, 1982).
2. Serra, J., Image Analysis and Mathematical Morphology, (Academic Press, London, 1982).
3. Sternberg, S. R., Computer Vision, Graphics, and Image Processing. 35, 333-335, 1986.
4. Haralick, R. M., Sternberg, S. R., Zhuang, X., IEEE Transactions on Pattern Analysis and Machine Intelligence. PAMI-9, 532-550, 1987.
5. Chackalackal, M. S., Basart, J. P., in preparation.
6. Skolnick, M. M., Computer Vision, Graphics, and Image Processing. 35, 306-332, 1986.
7. Meyer, F., Computer Vision, Graphics, and Image Processing. 35, 356-369, 1986.